Optimization of Background Information and Layer Thickness for Improved Accuracy of Water-Vapor Profile Retrieval from Ground-Based Microwave Radiometer Measurements at K-Band

Swaroop Sahoo, Xavier Bosch-Lluis, Steven C. Reising, *Senior Member, IEEE*, and Jothiram Vivekanandan, *Senior Member, IEEE*

***Abstract*—Ground-based microwave radiometers operating at frequencies near the 22.235 GHz (K-band) water vapor absorption line have been used extensively for remote sensing of water vapor in the troposphere, both the integrated amount and its profile. This paper explores the potential to use ground-based, zenith-pointing K-band radiometer measurements along with optimized background data sets consisting of radiosonde profiles to detect dynamic changes and gradients in water vapor profiles. To explore this capability, the HUMidity EXperiment 2011 (HUMEX11) was conducted at the U.S. Department of Energy's (DOE) Atmospheric Radiation Measurement (ARM) Southern Great Plains (SGP) Site near Lamont, OK, USA. This enables the choice of appropriate retrieval parameters to monitor temporal changes in atmospheric water vapor profiles. The results of this study illustrate that in a retrieval algorithm both the choice of the size of the background data set measured near the radiometer measurement time and the choice of atmospheric layer thickness affect the ability to remotely sense dynamic changes in water vapor. In general, it is found that background data sets of larger size provide better accuracy in a statistical sense but inhibit the ability to detect gradients.**

***Index Terms*—Atmospheric measurements, covariance matrix, humidity, microwave radiometry, remote sensing.**

I. Introduction

TRACKING dynamic changes in water vapor profiles is important to predict the timing and location of cloud formation as well as the initiation of convective storms. These storms develop on a time scale of 30–60 min in locations where the water vapor is highly variable [1]–[3]. Since convective initiation is highly sensitive to the amount of total column or, equivalently, precipitable water vapor (PWV), it is important to remotely sense PWV with fine temporal and spatial resolution. In particular, water vapor profile measurements with fine resolution in the planetary boundary layer are needed to analyze detailed, dynamic changes in the atmosphere [4].

Instruments used to measure water vapor profiles at present include radiosondes and Raman lidar, as well as microwave and infrared radiometers. Radiosondes provide water vapor measurements with fine vertical resolution (on the order of a few tens of meters) for the initialization of numerical weather prediction (NWP) models. However, the repeat time of radiosonde launches is not sufficient to track the dynamic evolution of tropospheric water vapor. Another instrument that can provide profile information to improve NWP models is Raman lidar [5]. These measurements have similar vertical resolution to that of radiosondes in the lowest 3 km of the troposphere and have temporal resolution of approximately 10 min [6]. Infrared radiometers, such as atmospheric emitted radiance interferometers (AERI), are useful for retrieval of water vapor and temperature profiles. Similarly, satellite-based microwave radiometer measurements are used to determine PWV, water vapor profiles, cloud liquid water, and wet path delay. Finally, ground-based microwave and millimeter-wave radiometers operate at frequencies near the water vapor absorption lines at 22.235 and 183.31 GHz to retrieve water vapor profiles [7], [8]. These instruments have fine temporal resolution; however, the accuracy of retrieved profiles varies depending on the retrieval algorithm and the thermodynamic parameter being retrieved. Westwater [9] described various retrieval techniques for estimation of water vapor and temperature profiles. Solheim *et al.* [10] compared the performance of various retrieval algorithms, i.e., Newtonian iteration method, regression method, neural networks, and Bayesian maximum probability estimation technique, for retrieval of water vapor, temperature, and liquid water profiles. Cimini *et al.* [7] and Hewison [11] focused on quantifying and improving the vertical resolution of retrieved water vapor and temperature profiles. Scheve and Swift [12] compared water vapor profiles retrieved from K-band microwave brightness temperature measurements to those retrieved from Raman lidar measurements.

In this work, water vapor profiles are retrieved from K-band radiometer measurements using Bayesian optimal estimation

Manuscript received January 03, 2014; revised August 13, 2014; accepted October 27, 2014. Date of publication February 23, 2015; date of current version December 21, 2015. This work was supported in part by the Center for Geosciences/Atmospheric Research, Cooperative Institute for Research in the Atmosphere, Colorado State University and in part by the U.S. National Aeronautics and Space Administration, Science Mission Directorate, Earth Science Technology Office, as part of the Instrument Incubator Program under Grant NNX11AH05G and Grant NNX14AK70G.

S. Sahoo, X. Bosch-Lluis, and S. C. Reising are with the Microwave Systems Laboratory, Department of Electrical and Computer Engineering, Colorado State University, Fort Collins, CO 80523 USA (e-mail: swaroop.sahoo@colostate.edu; xavier.bosch-lluis@colostate.edu; steven.reising@colostate.edu).

J. Vivekanandan is with the Earth Observing Laboratory, University Center for Atmospheric Research, Boulder, CO 80301 USA (e-mail: vivek@ucar.edu).

Color versions of one or more of the figures in this paper are available online at http://ieeexplore.ieee.org.

Digital Object Identifier 10.1109/JSTARS.2014.2370073

TABLE I
REQUIREMENTS BASED ON THE ALGORITHM THEORETICAL BASIS DOCUMENT FOR THE PLANNED BUT CANCELED NPOESS CMIS [14] AND FOR THE GROUND-BASED GPS NETWORK DEPLOYED AT THE ARM SGP SITE [31]

	Height above ground level	Water vapor uncertainty (in clear conditions)
NPOESS	From ground to 4 km	20% or 0.2 g/kg
	From 4 to 9 km	35% or 0.1 g/kg
GPS	From ground to 3 km	20% or 0.2 g/kg
	From 3 to 6 km	30–35% or 0.15 g/kg

[13] with an emphasis on detecting water vapor gradients in the lower troposphere that are dynamically evolving. For that purpose, background data sets of varying sizes are used to determine the statistical variability of atmospheric water vapor. The retrieved profiles are compared with water vapor profiles retrieved from a colocated Raman lidar. These Raman lidar measurements are assumed to be of high enough quality to be taken as "truth" for this study. Therefore, the error (i.e., deviation from "truth") is defined as the difference between a profile retrieved from microwave radiometer measurements and that retrieved from Raman lidar.

II. HUMIDITY EXPERIMENT 2011

The HUMidity EXperiment 2011 (HUMEX11) was conducted at the U.S. Department of Energy (DOE)'s Atmospheric Radiation Measurement (ARM) Southern Great Plains (SGP) Climate Research Facility in Lamont, OK, USA, for 3 weeks in the summer of 2011, during the periods of July 7–15 and August 3–15. This field campaign was designed to assess the ability to remotely sense dynamic changes and gradients in atmospheric water vapor profiles retrieved from K-band microwave brightness temperatures and to compare them with water vapor profiles retrieved from Raman lidar. Measurements were performed under various atmospheric conditions during clear skies, including stable conditions as well as rapidly evolving conditions shortly after rain showers in the area. The measurements were performed after a total rainfall of 12–40 mm over 6–12 h on certain days and when the water vapor density in the lowest 1 km above ground level (AGL) was between 8 and $19\,\mathrm{g/m^3}$. After precipitation events, the radiometer was operated after the sky was clear and clouds had moved out of the radiometer's field of view. Target accuracies for the retrievals were similar to the requirements shown in Table I for the planned National Polar-Orbiting Operational Environmental Satellite System (NPOESS) Conical-Scanning Microwave Imager/Sounder (CMIS), which was later canceled due to cost and schedule overruns [14].

During HUMEX11, two K-band, multifrequency Compact Microwave Radiometers for Humidity (CMR-H) profiling [15], [16] were deployed at the ARM SGP site. One of the two was colocated with a Raman lidar, enabling precise comparisons of profiles retrieved from the K-band brightness temperatures to those retrieved from the Raman lidar data. The other radiometer was deployed 10 km to the northwest, near Lamont, OK, USA. These microwave radiometers sampled atmospheric volumes using mechanical scanning over a range of both elevation and azimuth angles.

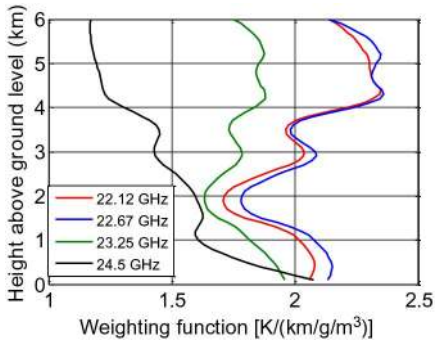

Fig. 1. Jacobian or weighting functions for the CMR-H frequencies.

The CMR-H K-band radiometers were developed at the Microwave Systems Laboratory (MSL) in the Electrical and Computer Engineering Department at Colorado State University (CSU) using monolithic microwave integrated circuit (MMIC) technology with low noise amplifier-based front ends [15]. The radiometers operate at four frequencies near the K-band water vapor absorption line, i.e., 22.12, 22.67, 23.25, and 24.5 GHz, with bandwidths of 110, 120, 120, and 200 MHz, respectively. Jacobians, or weighting functions, for these frequencies are shown in Fig. 1. The profile used to calculate these weighting functions is the average water vapor profile measured by radiosondes launched from the ARM SGP site on August 8, 2011. The radiometric resolution ($\mathrm{NE}\Delta\mathrm{T}$) of the CMR-H is 0.2 K for a 3-s integration time. The 3-dB antenna beamwidth for CMR-H is 3°–4°. The radiometer's system noise temperature at the four measurement frequencies is in the range of 550–800 K. The calibration precision at 298 K (while observing a microwave absorber at ambient temperature) is approximately 0.2 K for all four frequencies [15].

Calibration of the CMR-H brightness temperature measurements is performed by observing two objects of known brightness temperature. The "warm" calibration target is a microwave absorber at ambient temperature, and the "cold" calibration source is the cosmic microwave background temperature of 2.73 K at these frequencies, using tipping curve measurements extrapolated to zero atmospheres [17].

Furthermore, additional instruments were deployed at the ARM SGP site, including wind profilers [18], AERI [19], microwave radiometers [20]–[23], and *in situ* weather station sensors. Radiosondes were launched from the ARM SGP Central Facility every 6 h. This provides an opportunity to compare the retrieved results with data from other colocated instruments.

III. THEORETICAL DISCUSSION

Retrieval algorithms based on Bayesian optimal estimation have a number of inputs that influence the accuracy of their results. One of these is the background information covariance matrix, which describes the statistical variability of measured water vapor profiles over the time period during which they

occurred. It is calculated using a background data set, typically consisting of a collection of water vapor profiles measured over a certain period of time at a specific location. The number of elements in the background data set and the relationships among them determine the values of the background information covariance matrix elements, depending on whether they were measured during the day and/or night and in the same or different seasons. The importance of the size of the background data set and the retrieval algorithm used in this paper are discussed in detail in this section.

A. Initialization Profiles and Background Information

Water vapor profiles from various sources can be used as initialization profiles and background data, including *in situ* measurements from radiosondes and remote sensing measurements from Raman lidar, both of which have fine vertical resolution. Other potential sources of background data are statistical data sets and weather prediction model output compiled over a long time period, e.g., 1–3 years [9].

Radiosonde data have a typical vertical resolution of 10–20 m and therefore can detect fine gradients in the thermodynamic properties of the atmosphere, including water vapor in the lower troposphere. However, humidity biases in radiosonde measurements are often greater than 5% throughout the troposphere. Residual dry bias errors in radiosondes are greater during the day than the night by 5%–7% [24]. The radiosonde balloon typically takes 25–40 min to reach a height of 15–20 km AGL and may drift horizontally up to tens of km from the launch site [16], depending on the local wind speed and direction as it ascends.

Raman lidar measurements have a vertical resolution of 35 m from 0 to 0.2 km, 39 m from 0.2 to 3.7 km and 78 m from 3.7 to 6 km AGL [25] with a temporal resolution of 10 min. The relative humidity error in Raman lidar profiles is less than 10% for altitudes below 8.5 km [5] AGL.

The background data set for profile retrieval from radiometer measurements is typically high-vertical resolution radiosonde or remote sensing measurements [9] over a time period of 2–3 years. Background data sets are used to derive the statistics of profile variability, and their usefulness and applicability to retrievals depending upon the location at which and the time of the year during which they were measured. NWP model outputs are another potential source of background data. However, their spatial and temporal resolution may not be sufficiently fine to detect changes or sharp gradients in water vapor profiles [26].

B. Analysis Based on Background Information Covariance Matrix

In a general sense, the retrieval process performs a mapping between the measurement space and the retrieval solution space according to a probabilistic model in the presence of radiometric measurement noise, model inaccuracies, and representativeness errors [11]. To overcome these uncertainties, knowledge of variability (statistics) of the parameters in the solution space is required to retrieve the most probable state.

The Bayesian retrieval technique uses background statistics of the solution space to invert the measurement and retrieve the most probable solution, as illustrated by Cimini *et al.* [7] and Hewison [11] using the 1D-VAR technique as well as Löhnert *et al.* [27] using the integrated profiling technique. Specific retrieval algorithms that use Levenberg–Marquardt (LM) minimization [13] are based on Bayesian retrieval techniques and retrieve the most probable atmospheric state by considering both measurements and atmospheric background statistics.

The profile is retrieved based on four information sources [9], [13], [27]. The first two are the measured brightness temperature vector ($\bar{T}_B'$) and the covariance matrix of the background data set of water vapor ($\overline{\overline{S}}_a$). The third is the measurement error covariance matrix ($\overline{\overline{S}}_\varepsilon$), determined by the uncertainties of the measured brightness temperatures. The fourth is the Jacobian or weighting function matrix ($\overline{\overline{K}}$) [9], which is the sensitivity of the measured brightness temperatures to changes in atmospheric water vapor as a function of altitude AGL. Weighting functions depend on the operating frequency of each of the microwave radiometer channels and on the water vapor content and temperature of the atmosphere.

The quality of the retrieved profiles depends to a certain extent upon the second information source above, the water vapor background information covariance matrix [8]. Therefore, the size and content of the background data set from which the covariance matrix is calculated need to be systematically evaluated. Ideally, each element in the background data set is a sample of the same stationary process [28]. If so, the joint probability distribution of the atmospheric layers remains constant in time. Therefore, parameters such as the mean and covariance of each layer do not change depending on the size of the background data set after stabilization. Typically, the background data set is filtered based on location, season and time of day to ensure its stationarity [28]. Based on the central limit theorem, as its size increases, the background data set becomes a normally distributed random process describing a "mean" atmospheric behavior. However, failure to achieve stationarity introduces error into the retrieval since the prior statistics are not consistent with the atmospheric conditions at the time of the radiometer measurement and therefore will bias the retrievals.

Using a large background data set to determine the background information covariance matrix improves the description of the higher-order atmospheric statistics, which helps to improve the accuracy of retrieved water vapor profiles but also decreases the capability of retrieving or predicting singular (or so-called "outlier") events. This happens because the covariance matrix is general and therefore not "customized" for any particular atmospheric condition. The retrieval error approaches a constant value, but gradients or inversions in water vapor profiles will be difficult to detect with high accuracy since the covariance matrix describes the variability of water vapor profiles during the entire time period represented by the background data set. Therefore, both the content and size of the background data set are very important for the retrieval.

The goal of this work is to estimate water vapor profiles with acceptable accuracy (quantified in Table I) and atmospheric layer thickness, and also to be able to detect evolving changes

and gradients in atmospheric water vapor in the lowest 3 km of the troposphere. To this end, this part of the study focuses on optimization of the background data set size. In this case, the background information covariance matrix will not be general but instead will be particular to the current retrieval and will satisfy the requirement for stationarity, in the sense of a particular state of the atmosphere. Since the particular background data set does not describe every atmospheric condition, the retrieval performance is expected to degrade as a function of time between the initialization and the retrieval.

However, a small background data set (less than approximately 10 profiles) will not be able to describe the atmosphere accurately enough since it will not contain enough data to provide a sufficient statistical description. Taking this into consideration, it is reasonable to expect that the choice of optimum background data set size will be one of the factors determining the ability to detect evolving changes and gradients in water vapor profiles. The size of the background data set can be chosen based on the application. If the application is to monitor dynamic changes in water vapor profiles, a small data set can be chosen to correspond to recent weather conditions. Instead, if the application requires water vapor profiles with statistical or seasonal accuracy, a large background data set can be chosen, often collected over many months or years [9].

C. Retrieval Using the LM Algorithm

For the retrieval algorithm, the same LM optimization method has been used to estimate atmospheric water vapor as is used in the 1D-VAR [11]. The LM optimization method is similar to the Gauss–Newton (GN) optimization technique used in integrated profiling techniques [27] and in nonlinear inverse problems. LM is an iterative, nonlinear optimization algorithm, similar to the GN algorithm [27], [13] but with better performance for highly nonlinear problems. The main difference between LM and GN is that LM has a damping parameter γ that is updated during each iteration based on the ratio of the actual value of the cost function to that when the problem was considered to be linear. In the retrieval algorithm, the step sizes of the iteration for water vapor profiles are in the range of 0.01–0.1 $\mathrm{g/m^3}$. The LM algorithm usually converges within 15–20 iterations, similarly to the GN technique, and is shown as

$$\bar{\rho}_{i+1} = \bar{\rho}_i + \left((1+\gamma)\,\overline{\overline{S}}_a^{-1} + \overline{\overline{K}}_i^{T}\overline{\overline{S}}_\varepsilon^{-1}\overline{\overline{K}}_i\right)^{-1} \times \left(\overline{\overline{K}}_i^{T}\overline{\overline{S}}_\varepsilon^{-1}\left[\bar{T}'_B - \bar{T}_B(\bar{\rho}_i)\right] - \overline{\overline{S}}_a^{-1}\left[\bar{\rho}_i - \bar{\rho}_a\right]\right) \quad (1)$$

where

- i index of iteration;
- $\overline{\overline{K}}_i$ kernel function or weighting function matrix;
- γ LM factor;
- $\overline{\rho}$ water vapor density profile, where $\overline{\rho}_i$ is the initialization water vapor density profile when $i = 1$, and $\bar{T}'_B$ is the measured brightness temperature vector;
- $\overline{\rho}_a$ background profile, the same as the initialization profile. When the background data set is smaller than 150 profiles, a radiosonde profile taken close to the measurement time is used as the initialization profile;
- $\overline{T}_B$ simulated brightness temperature vector using a radiative transfer model for the four frequency channels of CMR-H. The Rosenkranz model is used to calculate the absorption coefficients used to simulate brightness temperatures;
- $\overline{\overline{S}}_\varepsilon$ measurement error covariance matrix of the CMR-H, where the main diagonal elements are equal to the radiometric resolution of each channel [29]. In this case, measurements at each of the frequencies are assumed to be independent of each other, so the off-diagonal elements have been assumed to be zero for this study. $\overline{\overline{S}}_\varepsilon$ also includes the noise in radiometric observations, representativeness error and radiative transfer model errors [11], [30];
- $\overline{\overline{S}}_a$ background information covariance matrix, with dimensions depending on the number of atmospheric layers used for the retrieval and with values based on the statistics of the background data set profiles.

LM is an iterative process in which the value of γ is chosen to minimize a cost function J, given by

$$J = \left(\bar{\rho} - \bar{\rho}^b\right)^T \overline{\overline{S}}_a^{-1}\left(\bar{\rho} - \bar{\rho}^b\right) + \left(\bar{T}_B\left(\bar{\rho}_i\right) - \bar{T}'_B\right)^T \overline{\overline{S}}_\varepsilon^{-1} \times \left(\bar{T}_B\left(\bar{\rho}_i\right) - \bar{T}'_B\right) \quad (2)$$

where $\bar{\rho}$ and $\bar{\rho}^b$ are the water vapor profile outputs for each iteration and initialization profile, respectively.

The value of γ at each iteration is adjusted based on the change in the value of the cost function J. The final output profile is chosen based on the convergence criterion given by [13]

$$\left[\bar{T}_B\left(\bar{\rho}_{i+1}\right) - \bar{T}_B\left(\bar{\rho}_i\right)\right]^T \overline{\overline{S}}_{\delta y}^{-1}\left[\bar{T}_B\left(\bar{\rho}_{i+1}\right) - \bar{T}_B\left(\bar{\rho}_i\right)\right] << m \quad (3)$$

where m is the number of measurements and $\overline{\overline{S}}_{\delta y}$ is the covariance between $\bar{T}'_B$ and $\bar{T}_B\left(\bar{\rho}_i\right)$. The iteration stops when (3) reaches a value k which is significantly less than m (where k is set at 0.04), and the resulting profiles are checked for consistency [11].

IV. Sensitivity of Retrieved Water Vapor Profiles

The atmospheric layer thickness and background data set size have a substantial effect on the root mean square (rms) error and on the ability to detect dynamic changes in the retrieved water vapor profiles.

A. Water Vapor Profile Retrievals for Different Layer Thicknesses

Retrievals were performed for 100-, 200-, 400-, and 500-m layer thicknesses using the data sources mentioned in Section III-A as well as the initialization profile. As alluded to in Section III, initialization profiles were obtained from

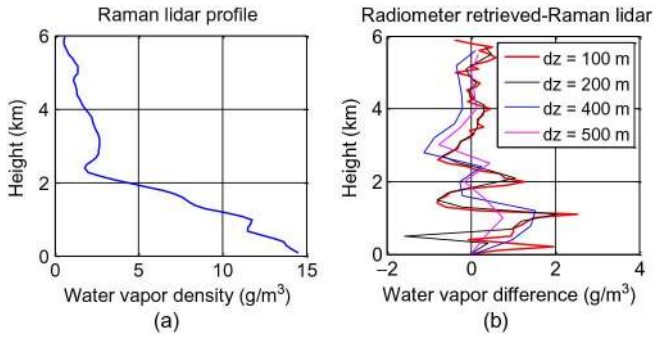

Fig. 2. (a) Raman lidar profile at 17:50 UTC on August 9, 2011; (b) difference between radiometer-retrieved and Raman lidar-retrieved profiles for 100-, 200-, 400-, and 500-m layer thicknesses.

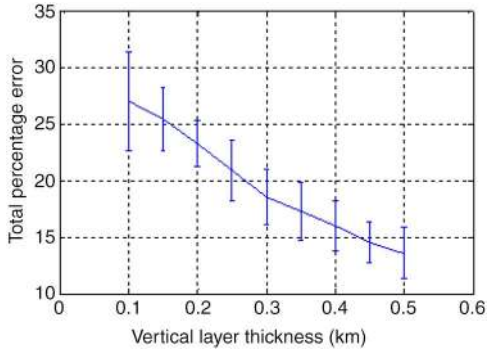

Fig. 3. Mean total percentage error in PWV (calculated as the difference between radiometer-retrieved and Raman lidar-retrieved water vapor profiles) as a function of layer thickness using 64 radiosonde observations as background information.

radiosonde data, with a typical vertical resolution of 10–20 m. The initialization profiles were vertically averaged to correspond to the layer thickness of the retrieval. For example, when using an initialization profile of 100-m layer thickness for the retrieval, the radiosonde water vapor profile was vertically averaged to 100 m.

The background data set consisted of measurements from 64 radiosondes that were launched during the daytime at the ARM SGP site during the months of July and August 2011. Radiosonde data from these 2 months were used as two separate background data sets for retrievals during each of the two respective months. Results described in Sections IV-A–IV-C are for 40 retrieved profiles using measurements performed over 3 weeks during the field experiment. These profiles were retrieved using various layer thicknesses and compared with Raman lidar profiles to quantify the rms error for each of them. Fig. 2(a) shows a profile retrieved for August 9, 2011 at 17:50 UTC from Raman lidar measurements, and Fig. 2(b) shows the associated difference between radiometer-retrieved and Raman lidar-retrieved profiles for 100-, 200-, 400-, and 500-m layer thicknesses. Data from a radiosonde launched at 16:30 UTC are used as the *a priori* for the retrieval of each water vapor profile from the radiometer measurements. Ground-based *in situ* measurements were used throughout this study to constrain the surface temperature, humidity and pressure for the retrieved profile.

To calculate the error as a function of height, the Raman lidar-retrieved values have been averaged to the same vertical layer thickness as the radiometer estimates. Fig. 2(b) shows that the difference between the radiometer-retrieved and Raman lidar-retrieved profiles is larger than $1\,\mathrm{g/m^3}$ for layer thicknesses of 100 and 200 m in the lowest 2.2 km of the troposphere. This difference decreases with increasing altitude AGL. As the layer thickness is increased, the difference decreases as well. The profiles with 400- and 500-m layer thicknesses significantly smooth out the vertical variations in the water vapor profile, thereby reducing the error.

The errors in the retrieved profile with respect to the Raman lidar profile averaged over the lowest 3 km of the troposphere, i.e., the most significant part of the atmosphere in terms of water vapor variability, are 19.3%, 16.7%, 13.9%, and 8.2% for 100-, 200-, 400-, and 500-m layer thicknesses, respectively. The total error of a profile (hereafter "total percentage error in PWV") was determined as the sum of the absolute values of errors at all levels up to and including 6-km AGL. The total errors of 40 estimated profiles are used to determine the mean and standard deviation of the total percentage error for each layer thickness from 100 to 500 m in 50-m increments. The results are shown in Fig. 3. As the layer thickness increases from 100 to 500 m, the mean total percentage error decreases from 27% to 13% and the standard deviation decreases from 4.5% to 2.3%. Fig. 3 shows an inverse relationship between the layer thickness and the total percentage error. In other words, the thinner the atmospheric layers are, the greater the overall estimation error is.

The accuracy of retrieved profiles depends to a great extent on the quality of the initialization profile, background information, and measurement error covariance matrices. Typically, the retrieved profile follows the trend of the initialization profile. If the initialization profile (here the radiosonde profile used for the retrieval) is substantially different from the actual water vapor profile, the error of the retrieved profile will be large. In that case, the retrieval process might not be able to capture gradients or aspects of the actual water vapor profile. So, the initialization profile needs to have statistical properties that are similar to those of the actual profile.

B. Variation in Predictability With Change in Background Data Set Size and Atmospheric Layer Thickness

The retrieval accuracy has been evaluated based on the mean and standard deviation of total percentage error in the retrieved water vapor profiles for background data set sizes ranging from 2 to 110 profiles. A background data set containing less than 10 profiles does not have sufficient statistical significance, but the analysis has been performed to improve understanding of its impact on the retrieval. The covariance matrices were calculated using background data sets containing 2 to 110 profiles with an increment of two. Each increment added one profile taken before the measurement and one taken after. These profiles were chosen to be as close to the time of measurement as possible. For example, for the radiometer measurement at 14:00 UTC on August 8, 2011, the two radiosonde profiles chosen were at 12:00 UTC and at 18:00 UTC on August 8, 2011. The

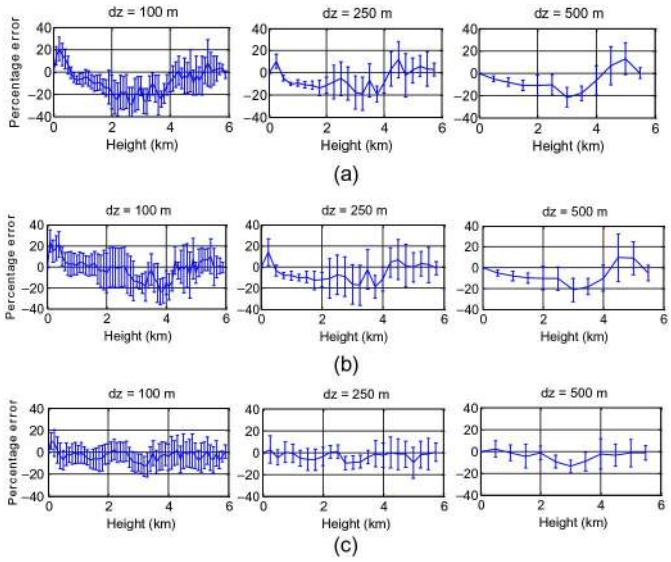

Fig. 4. Mean and standard deviation of percentage error of radiometer-retrieved profiles with respect to Raman lidar-retrieved water vapor profiles for 100-, 250-, and 500-m layer thicknesses and background data set sizes of (a) 16 elements; (b) 32 elements; and (c) 64 elements.

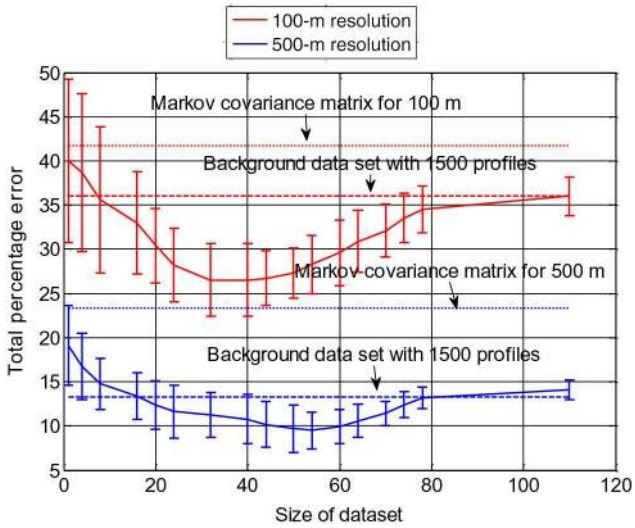

Fig. 5. Mean total percentage error and its standard deviation for retrieved profiles (for layer thicknesses of 100 and 500 m) as a function of the size of the background data set. The total percentage errors for a background data set size of 1500 (for layer thicknesses of 100 and 500 m) are shown by the long dashed red and blue horizontal lines at 36% and 13%, respectively.

radiosondes were launched four times daily at 0, 6, 12, and 18 UTC. If two additional profiles were added to the data set, to use similar times of day to represent diurnal conditions similar to when the radiometer measurement was taken, they would be at 18:00 UTC on August 7, 2011, and at 12:00 UTC on August 9, 2011, and so on. This method of choosing an equal number of radisonde profiles before and after the retrieval time is particularly applicable to this study. This would not be possible if the radiometer measurements were used to retrieve water vapor profiles on a real-time basis. In that case, only radiosonde profiles taken before the retrieval time would be available for use as the background data set.

For small background data set sizes, the time interval between initialization profile and retrieved profile has a substantial impact on the retrieval accuracy. The ability to detect changes in retrieved water vapor profiles is partially determined by the size of the background data set used and by the quality and applicability of the *a priori*. The accuracy depends to a certain extent on the background data set size and also on the time interval between the radiometer measurement and the radiosonde profiles in the background data set, as well as the layer thickness used for the retrieval. Therefore, the accuracy of the retrieval for a variety of background data set sizes is analyzed for varying layer thicknesses. This analysis involved using a background data set taken close in time to the radiometer measurement so that the background information covariance matrix would be representative of the variability near this time.

As before, water vapor profiles were retrieved for 40 measurement times while varying the layer thickness from 100 to 500 m as well as the size of the background information covariance matrix from 2 to 110. Fig. 4(a)–(c) shows the mean error and its standard deviation calculated using 40 retrievals for data set sizes of 16, 32, and 64, respectively, and layer thicknesses of 100 m (left panel), 250 m (middle panel), and 500 m (right panel). The curve and error bars represent the mean (bias) error and its standard deviation, respectively. Fig. 4 shows that, for any particular layer thickness studied, as the size of the background data set increases, the bias of the retrieval decreases. For any particular background data set, as the layer thickness increases, the uncertainty of retrieval also decreases. In addition, there is an optimum background data set size for minimum standard deviation. The bias is related to the mean error, and the standard deviation is related to the uncertainty of the retrieval. Fig. 4 shows that the results are consistent with the qualitative discussion in Section III-B.

C. Change in Total Percentage Error With Change in Background Data Set Size

This study was performed to find the optimal background data set size to minimize the total percentage error while maintaining the ability to detect changes in the gradients of the water vapor profile. The total percentage errors were calculated for retrievals using each background data set size, where the background data set was taken close to the radiometer measurement time. The mean and standard deviation of percentage errors for data set sizes from 2 to 110 (as well as 1500) are shown in Fig. 5 as red and blue curves for layer thicknesses of 100 and 500 m, respectively.

1) Total Percentage Error for 100-m Layer Thickness: Fig. 5 shows that for a 100-m layer thickness and a background data set size of four, the total percentage error is 38.5%. Although the background covariance matrix calculated from a data set of four profiles is not statistically significant, it has been included in the study for completeness. The mean total error decreases as the background data set size increases and reaches a minimum of 27% for a background data set size of 40. This is because the retrieved profiles are stationary with

respect to the background data set of 40 profiles, and the background data set is related to the current atmosphere. When the size of the background data set taken close in time to the radiometer measurement is 40, it is inferred from the minimum error that the statistics used in the covariance matrix agree with the variability associated with the actual water vapor profile. Throughout Fig. 5, the standard deviation associated with each total percentage error is shown by the error bars. The total error increases when the background data set size is greater than 40 because the retrieved profile is no longer stationary with respect to the background data set; the *a priori* statistics do not describe the water vapor profile accurately since the background atmospheric conditions have changed.

When the background data set size is larger than 40, the weather conditions associated with the background data set are different from those during the radiometer measurement. For a background data set size larger than a certain threshold, i.e., 1500 profiles as shown in Fig. 5, the mean error becomes nearly constant at 36% mean total error, as shown by the long-dashed red horizontal line. Similarly, when a Markov covariance matrix, which emulates a synthetic atmosphere [13], is used as a background information matrix, the mean error is 42%, as shown by the short-dashed red horizontal line. The total error would not have this trend if the selected data set for background covariance matrix calculation was not related to the atmospheric condition during the measurement.

2) Total Percentage Error for 500-m Layer Thickness: Similar to Section IV-C1, Fig. 5 shows that the error for 500-m layer thickness and a background data set size of four has a total percentage error of 17%, while the background covariance matrix for a data set size of four is not statistically significant but is used for completeness. The error decreases as the background data set size increases until it reaches a minimum of 9% for a background data set size of 50–55. After the total error reaches a minimum, it then begins to increase as the number of profiles in the background data set increases. The error becomes nearly constant at 13% (as shown in the long-dashed blue horizontal line) for a background data set size of 1500 or greater, due to the stationarity effect discussed in Section IV-C1. The mean error using a Markov covariance matrix as the background covariance matrix for 500-m layer thickness is 23%, as shown by the short-dashed blue horizontal line. It is important to observe that the retrieval errors for 500-m thick layers are lower than for 100-m thick layers. However, the retrieval for 500-m layer thickness not only averages the error associated with the retrieval but also averages the important information about dynamic changes. To retrieve information about dynamic changes, it is better to use 100-m layers instead of 500-m layers.

A similar analysis was performed by using a background data set from September 2008, and the background data set size was varied from 2 to 110 to determine the total mean error. The results of this analysis are shown in the red curve in Fig. 6 for 500-m layer thickness. The mean total errors are substantially larger than those when the background data set is taken close to the measurement time during July and August of 2011. This is because the background data set taken from 2008 is not stationary with the atmospheric water vapor during the radiometer measurement. The difference between the errors in Fig. 6 is largest at 16% for a background data set size of four and decreases as the background data set size is increased. The difference is smallest when the background data set size is larger than 110 profiles. This is because the variability between data sets of four profiles taken at two different times is very different. However, the variability between data sets of 110 profiles taken at two different times tends to be quite similar.

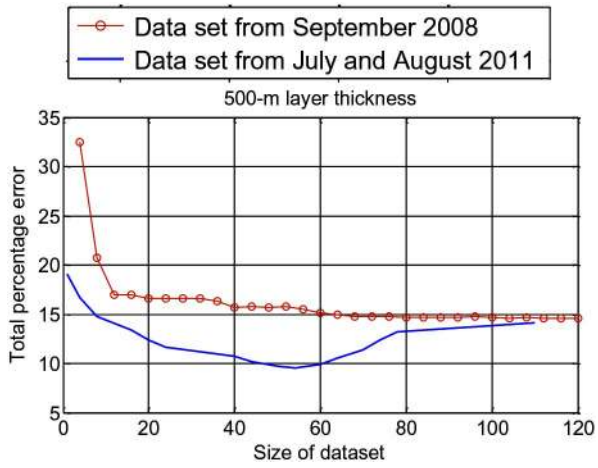

Fig. 6. Mean total percentage error for retrieved profile (for layer thickness of 500 m) as a function of the size of the background data set.

3) Analysis of Variability Content Associated With Background Information Covariance Matrix: The covariance matrix ($\overline{\overline{S}}_a$) is computed using

$$\overline{\overline{S}}_a = E\left(\overline{\overline{A}} - \left\langle\overline{\overline{A}}\right\rangle\right)\left(\overline{\overline{A}} - \left\langle\overline{\overline{A}}\right\rangle\right)^T \tag{4}$$

where $\overline{\overline{A}}$ is the background data set and $\langle\overline{\overline{A}}\rangle$ represents the mean profile computed from the background data set. The matrix $\overline{\overline{S}}_a$ has dimensions of $N \times N$, where N is the number of layers (vertical levels) regardless of the number of profiles that have been used to calculate it (in this study, $N = 60$ for 100-m and $N = 12$ for 500-m layer thicknesses). As the size of the background data set is increased, the values of the elements of $\overline{\overline{S}}_a$ also change. Fig. 7 shows the $\overline{\overline{S}}_a$ for 100-m layer thickness using background data sets with 2, 40, 64, and 1000 profiles.

An eigenvalue analysis [10] of the background information covariance matrix was performed to determine its variability content for the purpose of detecting dynamic changes in water vapor profiles while minimizing the error. For the eigenvalue analysis, the length of $\overline{\overline{A}}$ is increased from 2 to 110 using the background data set measured during HUMEX11, and $\overline{\overline{S}}_a$ is calculated for each background data set ($\overline{\overline{A}}$) size. The eigenvalue analysis of the covariance matrix corresponding to each background data set gives a vector of N eigenvalues. When the background data set size is varied from 2 to 110, it results in 109 vectors of N eigenvalues each.

The results presented here show the normalized eigenvalue trajectory [12] for the covariance matrices for layer thicknesses of 100 and 500 m in Fig. 8(a) and (b), respectively.

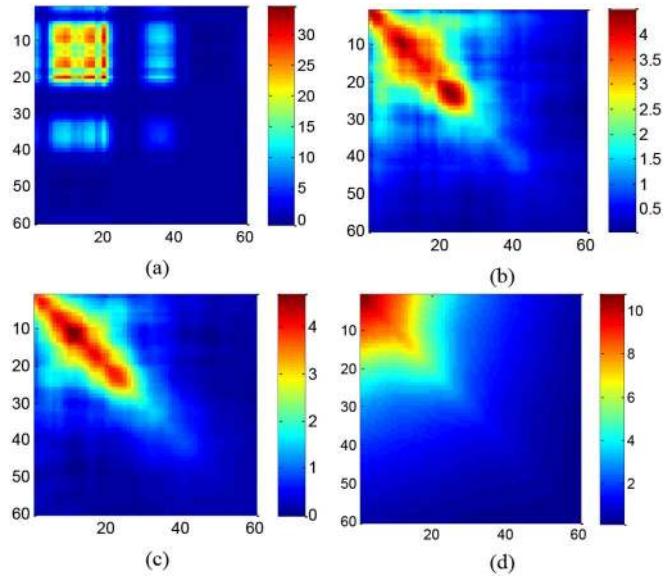

Fig. 7. Covariance matrix ($\overline{\overline{S}}_a$) calculated for 100-m layers ($N = 60$) using (a) 2 profiles; (b) 40 profiles; (c) 64 profiles; and (d) 1000 profiles.

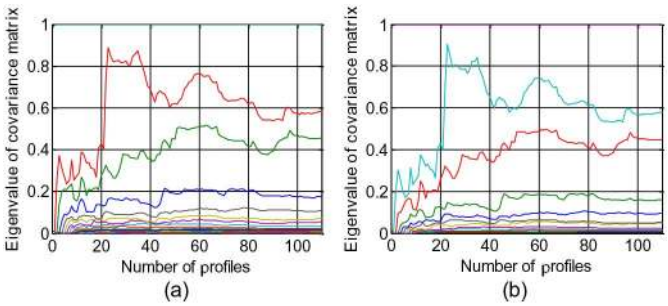

Fig. 8. Eigenvalue analysis of the data set as the number of water vapor profiles is increased from 2 to 110 for layer thicknesses of (a) 100 m and (b) 500 m. The red curve in (a) represents the trajectory of a normalized eigenvalue as the number of profiles is increased from 2 to 110. Each curve represents the trajectory of a different normalized eigenvalue.

The number of curves corresponds to the N layers in the retrieval, while each curve extends from 2 to 110, i.e., the number of profiles used to calculate $\overline{\overline{S}}_a$. Trajectories of each curve represent the evolution of the eigenvalues as the background data set size increases, where each curve [e.g., red, green, and blue curves in Fig. 8(a)] represents the trajectory of an individual normalized eigenvalue as the number of profiles is increased from 2 to 110. In Fig. 8, as the number of water vapor profiles in the background data set is increased, the largest eigenvalue increases and reaches a maximum at approximately 25–35 and remains above 0.8 for about 35 new profiles thereafter, for both 100- and 500-m layer thicknesses.

A similar eigenvalue analysis was performed using 1400 water vapor profiles as a background data set for calculating the background information covariance matrix. This data set included radiosonde launches from the same location during 2008 and 2009 corresponding to different weather conditions than during HUMEX11. The normalized eigenvalue analysis results are shown in Fig. 9. It should be noted that the maximum value is 0.3 for a background data set size of 35–40. The

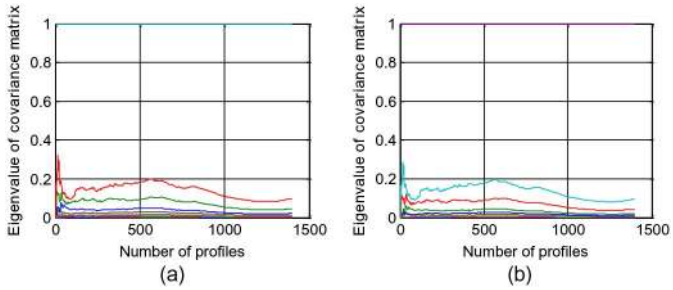

Fig. 9. Eigenvalue analysis of the data set as the number of water vapor profiles is increased from 2 to 1400 for layer thicknesses of (a) 100 m and (b) 500 m. The red curve in (a) represents the trajectory of a normalized eigenvalue as the number of profiles is increased from 2 to 1400.

maximum eigenvalue is substantially lower than that in Fig. 8. However, the optimum data set size (the data set that contains the most variability) is still similar to that in Fig. 8. Increasing the number of profiles for calculating the background covariance matrix increases the accuracy of the retrieval (average profile) until the number of profiles in the background data set reaches 500.

In this work, the eigenvalues are a measure of the variability associated with the background covariance matrix ($\overline{\overline{S}}_a$) used for the retrieval algorithm. In that case, the number of profiles used to calculate $\overline{\overline{S}}_a$ at which the eigenvalues reach a maximum value has two interpretations.

1) The background data set is correlated with the atmospheric state during the radiometric measurement time, e.g., in Fig. 8 profiles are close in time to the retrieval, and the peak indicates maximum variability according to the current atmosphere, which will provide a better retrieval. It is clear from the results that when a background data set with fewer than 10 profiles is used, it does not have enough statistical significance and the retrieval error is high, as shown in Fig. 5. However, when the data set is in the range of 40–60 profiles that have been taken close to the measurement time (as shown in Figs. 5 and 6), it provides information about the variability of the water vapor profile during the radiometric measurement. Therefore, the retrieval will be useful for detecting dynamic changes, as shown in Figs. 5 and 6.
2) The background data set is not correlated with the atmospheric state during the measurement time. In Fig. 9, the maximum would be considered "noise," i.e., atmospheric fluctuations that are not related to the radiometric observations. In this case, the best option is to perform the retrieval when the data set has enough significance and the values of the eigenvalues are low (i.e., the size of the data set needs to be large). Using a large data set has the effect of averaging out the variability of the atmosphere (smoothing), as shown in Fig. 7(d) for 1000 profiles. In that case, the retrieval will tend toward a "standard atmosphere," and the retrieval algorithm will have good performance when measuring a "standard atmosphere," i.e., the information contained in $\overline{\overline{S}}_a$. However, the retrieval will have difficulty detecting dynamic changes in water

vapor because $\overline{\overline{S}}_a$ does not contain the necessary information to do so. This is where the distinction between the retrieval accuracy and the ability to detect dynamic changes is meaningful, i.e., to distinguish between these two types of effects.

Therefore, as shown in Fig. 8, a background data set size of 25–35 provides maximum information about the variability of water vapor profiles. For a background data set size greater than 100 profiles, the eigenvalues of the covariance matrix are nearly constant as the background data set size changes; therefore, additional profiles provide no new information about water vapor variability. However, there is a noticeable discrepancy between the eigenvalue peak at a background data set size of 25–35 (in Fig. 8), and the minimum total error obtained (from Fig. 5), which occurs at a background data set size of 40–55. This is because a balance exists between the variability associated with the $\overline{\overline{S}}_a$ matrix and its significance. This means that the maximum information is provided by using 25–35 profiles in the background data set (from Fig. 8). However, this data set is not sufficiently large to provide the optimum information about water vapor variability in the atmosphere to minimize the error of the retrieval.

As already mentioned in the theoretical discussion of the background information covariance matrix in Section III-B, the number of independent vectors in the covariance matrix obtained using only two profiles [Fig. 7(a)] is similar to one, which is clear from the vertical and horizontal patterns (most of the rows and columns of the matrix are scaled versions of the same vector). Therefore, all N eigenvalue trajectories start at zero, which corresponds to eigenvalues for a background data set with two profiles. This is due to the fact that limited information will be obtained when calculating the covariance matrix of two consecutive atmospheric profiles since the atmosphere does not change significantly between the times at which two consecutive radiosondes are launched. As a result, the retrieval has poor performance when using a small number of background profiles. It is evident that this $\overline{\overline{S}}_a$ is not statistically significant and is not useful for retrievals, but it has been analyzed for completeness of the study. On the other hand, when the number of profiles in the background data set increases [as in Fig. 7(b) and (c)], the vertical and horizontal patterns disappear (although the covariance matrix has diagonal symmetry). This improvement results from increasing the number of profiles, which takes into account more states of the atmosphere, so the values of the N eigenvalues, as well as the number of linearly independent vectors, increase. Increasing the number of profiles in the background data set used for computing $\overline{\overline{S}}_a$ above a certain value causes the vertical and horizontal patterns to reappear [as in Fig. 7(d)], with a consequent reduction in the number of linearly independent vectors (or information about water vapor variability). It can be observed that the difference between the $\overline{\overline{S}}_a$ for 40 profiles [Fig. 7(b)] and that for 1000 profiles [Fig. 7(d)] has a substantial impact on the quality of the retrieval. Using the $\overline{\overline{S}}_a$ in Fig. 7(b) results in the retrieval assigning more variability to the layers at 2–3 km altitude, while using the $\overline{\overline{S}}_a$ in Fig. 7(d) results in assigning more variability to the lower layers at 0–1 km altitude. Therefore, there is a substantial difference between results using $\overline{\overline{S}}_a$ calculated using 40 and 1000 profiles.

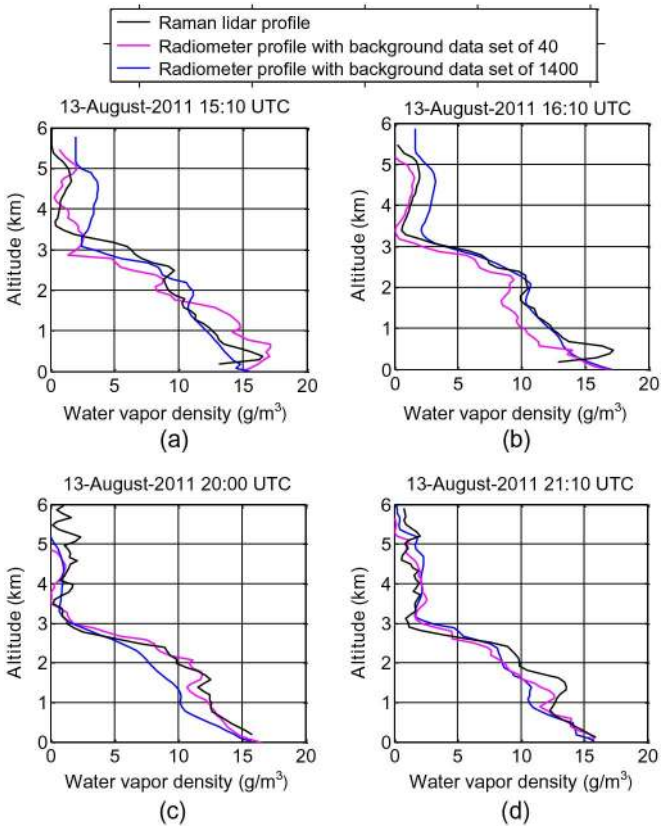

Fig. 10. Time series of retrieved water vapor profiles for 100-m layer thickness and background data set sizes of 40 and 1400, in comparison with Raman lidar profiles.

From the total percentage error analysis in Fig. 5 and the eigenvalue analysis of the background data covariance matrix in Figs. 8 and 9, it has been confirmed that the optimum size of background data set is approximately 40 and 60 for 100- and 500-m layer thicknesses, respectively. However, these specific optimum sizes can change for different layer thicknesses, time, location, background statistics (*a priori* profile and background error covariance), and season of retrieval.

To determine the ability to sense dynamic changes in water vapor profiles, retrievals from radiometer measurements were performed for 100-m layer thickness and background data set sizes of 40 and 1400 profiles. Results of the retrieval for August 13, 2011 are shown in Fig. 10, in which they are compared with Raman lidar-retrieved profiles. The profiles retrieved using a background data set size of 40 profiles (pink curves) track the inversions in the humidity profile at 500–600 m at 15:10 UTC and at 1300–1600 m at 21:10 UTC. Similarly, the slight inversion at 1400–1600 m at 20:00 UTC is also detected. However, the profiles retrieved using background data set sizes of 1400 profiles (blue curves) follow a trend generally similar to the Raman lidar-retrieved profiles but do not include the fine gradients and inversions in the lowest 2 km of the troposphere.

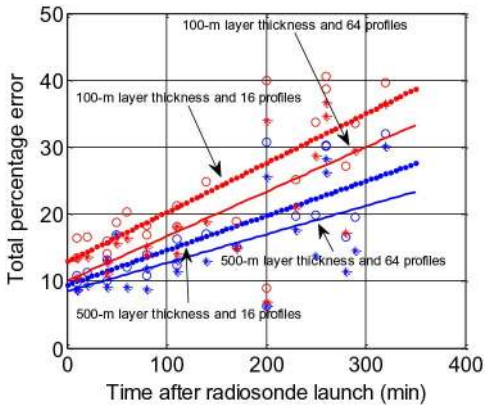

Fig. 11. Total percentage error as a function of time between radiosonde launch and radiometer measurement for 100- and 500-m layer thicknesses as well as background data set sizes of 16 and 64.

These results show that the retrieval using a background data set size of approximately 40 profiles for 100-m layer thickness is optimal in this case to retrieve water vapor profiles and also detect the gradients. However, this background data set of 40 profiles applies to weather conditions during the HUMEX11 experiment. The optimal number of profiles might be different for other weather conditions and locations.

V. Variation in Accuracy With Time Between Initialization Profile and Measurement

The retrieval accuracy varies significantly with respect to the time interval between initialization profile (from radiosondes) and the radiometer measurement. This is particularly evident for small background data set sizes (in the range of 50–100 profiles) to detect evolving changes in atmospheric water vapor profiles.

Retrievals were performed and errors were calculated for two layer thicknesses of 100 and 500 m for each retrieval time and background data set sizes of 16 and 64. As shown in Fig. 11, the errors were computed for 40 radiometer measurements as a function of time after the corresponding radiosonde launch. The total percentage error at 500-m vertical layer thickness is lower than that at 100-m layer thickness for most cases.

Total errors are minimum when the radiometer measurements are close in time to the radiosonde launches. This is because the shape and values of the initialization profile are similar to those of the actual atmospheric profile at the retrieval time. Total errors for 500- and 100-m vertical layer thickness are in the range of 7%–15% and 12%–22%, respectively, for a time range of 0–150 min after the radiosonde launch (for background data set size of 64). Retrievals for 100-m layer thickness which are the longest in time (4–5 h) after the radiosonde launches have errors in the range of 22%–30%. The largest error corresponds to 100-m layer thickness and a background data set size of 16. Conversely, the smallest error corresponds to the 500-m layer thickness with background data set size of 64. As shown in Fig. 11, as radiometer measurements are performed longer in time after the radiosonde launch, the percentage error increases. The errors are still less than the errors shown in Table I when the *a priori* data used for the retrieval are taken within 150 min of the radiometer measurement time. Finally, the likelihood of sensing dynamic changes and gradients in the water vapor profile decreases as the elapsed time since the launch of the most recent radiosonde.

VI. Summary and Discussion

Various analyses have been performed to show that the size of the background data set as well as the layer thickness in a retrieval play an important role in determining the accuracy of estimated profile and the ability of the retrieval to sense dynamic changes. This particularly applies to the case when the background data set is correlated with the atmospheric state during the radiometric measurement, i.e., profiles that have been taken close in time and that represent the variability associated with the actual water vapor profile during the radiometric measurement. Therefore, there exists an optimal background data set size which provides minimum retrieval error. On the contrary, if a background data set taken close in time to the radiometric measurement is not available, the best performance is obtained by using a large background data set taken over a long period of time representing seasonal variability. This makes the retrieval tend toward a "standard atmosphere."

Eigenvalue analysis of the covariance matrix for data set sizes of 110 and 1400 profiles for both 100- and 500-m layer thicknesses show that maximum variability occurs for data set sizes of approximately 25–35 profiles. However, the maximum accuracy is achieved by using a data set of 40–60 profiles. Therefore, there is a balance between the ability to achieve maximum accuracy and to use a background data set with maximum variability, to provide the maximum amount of information to sense dynamic changes. This is because the variability of a background data set can be associated not only with dynamic changes in the atmosphere but also with noise. To reduce the effect of noise, it is necessary for the background data set to have statistical significance. Normally, this is achieved by increasing the data set size to greater than 25–35 profiles. Therefore, the optimal background data set for minimal retrieval error has to be short enough to be close in time to the measurements but long enough to be statistically significant.

Under the assumption that the background data set is correlated with the atmospheric state during the radiometric measurements, both the eigenvalue analysis and accuracy show that continuing to increase the data set size above a certain value does not improve the retrieval accuracy. Instead, additional profiles provide information on the average state of the atmosphere. Large background data sets provide better accuracy in a statistical sense, but dynamic changes cannot be detected. Therefore, a large background data set is less than optimal for sensing dynamic changes in the atmosphere.

In this study, water vapor profiles retrieved from radiometer measurements have confirmed that retrievals using thin atmospheric layers and an optimal background data set size taken close to the measurement time have a greater likelihood of sensing dynamically evolving changes in water vapor profiles than larger background data sets do with thicker layers. Therefore, optimum background data set sizes with thin atmospheric layers

can be used to retrieve water vapor profiles on days when the weather is evolving rapidly, while large background data sets with thicker layer can be used when the weather is more nearly constant in time. Therefore, depending on the weather conditions, background data set sizes and layer thicknesses can be chosen appropriately.

ACKNOWLEDGMENT

The authors would like to thank the Department of Defense/Colorado State University Center for Geosciences and Atmospheric Research (CG/AR) for sponsoring this field experiment and the Department of Energy's Atmospheric Radiation Measurement Southern Great Plains site personnel for their assistance during the HUMEX11 field experiment. They would also like to thank the NASA Earth Science Technology Office for partial support of the data analysis, and I. Thakkar and S. Nelson for supporting the microwave radiometer measurements during the HUMEX11 field experiment.

REFERENCES

[1] M. N. Deeter and K. F. Evans, "Mesoscale variations of water vapor inferred from millimeter-wave imaging radiometer during TOGA COARE," *J. Appl. Meteorol.*, vol. 36, no. 2, pp. 183–188, Feb. 1997.

[2] H. Seko, H. Nakamura, Y. Shoji, and T. Iwabuchi, "The meso-gamma scale water vapor distribution associated with thunderstorm calculated from a dense network of GPS receivers," *J. Meteorol. Soc. Jpn*, vol. 82, no. 1B, pp. 569–586, Mar. 2004.

[3] D. H. Lenschow and B. B. Stankov, "Length scales in the convective boundary layer," *J. Atmos. Sci.*, vol. 43, no. 12, pp. 1198–1209, Jun. 1986.

[4] National Research Council Committee on Developing Mesoscale Meteorological Observational Capabilities to Meet Multiple National Needs, *Observing Weather and Climate from the Ground Up: A Nationwide Network of Networks*. Washington, DC, USA: Nat. Acad. Press, 2009.

[5] R. A. Ferrare *et al.*, "Evaluation of daytime measurements of aerosols and water vapor made by an operational Raman lidar over the Southern Great Plains," *J. Geophys. Res.*, vol. 111, no. D05S08, pp. 1–21, 2006, doi: 10.1029/2005JD005836.

[6] R. K. Newsom, *Raman Lidar (RL) Handbook*, U.S. Dept. Energy, Office Sci., Office Biol. Environ. Res., 2009 [Online]. Available: http://www.arm.gov/publications/tech_reports/handbooks/rl_handbook.pdf?id=89

[7] D. Cimini, T. J. Hewison, L. Martin, J. Güldner, and F. S. Marzano, "Temperature and humidity profile retrievals from groundbased microwave radiometers during TUC," *Meteor. Z.*, vol. 15, no. 5, pp. 45–56, Feb. 2006.

[8] D. Cimini, E. R. Westwater, and A. J. Gasiewski, "Temperature and humidity profiling in the arctic using millimeter-wave radiometry and 1DVAR," *IEEE Trans. Geosci. Remote Sens.*, vol. 48, no. 3, pp. 1381–1388, Mar. 2010.

[9] E. R. Westwater, "Ground-based microwave remote sensing of meteorological variables," in *Atmospheric Remote Sensing by Microwave Radiometry*. Hoboken, NJ, USA: Wiley, 1993, pp. 145–214.

[10] F. S. Solheim *et al.*, "Radiometric profiling of temperature, water vapor, and cloud liquid water using various inversion methods," *Radio Sci.*, vol. 33, pp. 393–404, 1998.

[11] T. J. Hewison, "1D-VAR retrieval of temperature and humidity profiles from a ground-based microwave radiometer," *IEEE Trans. Geosci. Remote Sens.*, vol. 45, no. 7, pp. 2163–2168, Jul. 2007.

[12] T. M. Scheve and C. T. Swift, "Profiling atmospheric water vapor with a K-band spectral radiometer," *IEEE Trans. Geosci. Remote Sens.*, vol. 37, no. 3, pp. 1719–1729, May 1999.

[13] C. D. Rodgers, *Inverse Methods for Atmospheric Sounding: Theory and Practice*. Singapore: World Scientific, 2000.

[14] Atmospheric, and Environmental Research, Inc. (2001, Mar. 15). *Algorithm Theoretical Basis Document (ATBD) for the Conical-Scanning Microwave Imager/Sounder (CMIS) Environmental Data Records (EDRs)* [Online]. Available: https://www.aer.com/sites/default/files/atbd_v07-1_CIWP.pdf, accessed on May 15, 2014.

[15] F. Iturbide-Sanchez, S. C. Reising, and S. Padmanabhan, "A miniaturized spectrometer radiometer based on MMIC technology for tropospheric water vapor profiling," *IEEE Trans. Geosci. Remote Sens.*, vol. 44, no. 7, pp. 2181–2193, Jul. 2007.

[16] S. Padmanabhan, S. C. Reising, J. Vivekanandan, and F. Iturbide-Sanchez, "Retrieval of atmospheric water vapor density with fine spatial resolution using 3-D tomographic inversion of microwave brightness temperatures measured by a network of scanning compact radiometers," *IEEE Trans. Geosci. Remote Sens.*, vol. 47, no. 11, pp. 3708–3721, Nov. 2009.

[17] Y. Han and E. R. Westwater, "Analysis and improvement of tipping calibration for ground-based microwave radiometers," *IEEE Trans. Geosci. Remote Sens.*, vol. 38, no. 3, pp. 1260–1277, May 2000.

[18] W. L. Ecklund, D. A. Carter, and B. B. Balsley, "A UHF wind profiler for the boundary layer: Brief description and initial results," *J. Atmos. Ocean. Technol.*, vol. 5, pp. 432–441, 1988.

[19] W. F. Feltz, H. B. Howell, R. O. Knuteson, H. M. Woolf, and H. E. Revercomb, "Near continuous profiling of temperature, moisture, and atmospheric stability using the Atmospheric Emitted Radiance Interferometer (AERI)," *J. Appl. Meteorol.*, vol. 42, pp. 584–597, 2003.

[20] M. Decker, E. Westwater, and F. Guiraud, "Experimental evaluation of ground-based microwave sensing of atmospheric temperature and water vapor profile," *J. Appl. Meteorol.*, vol. 17, no. 12, pp. 1788–1795, Dec. 1978.

[21] M. P. Cadeddu. (2012, May 01). *Microwave Radiometer—3 Channel (MWR3C) Handbook* [Online]. Available: http://www.arm.gov/publications/tech_reports/handbooks/mwr3c_handbook.pdf?id=24, accessed on May 15, 2014.

[22] V. R. Morris. (2006, Aug.). *Microwave Radiometer (MWR) Handbook* [Online]. Available: http://www.arm.gov/publications/tech_reports/handbooks/mwr_handbook.pdf?id=36, accessed on May 15, 2014.

[23] M. P. Cadeddu, J. C. Liljegren, and D. D. Turner, "The Atmospheric Radiation Measurement (ARM) Program network of microwave radiometers: Instrumentation, data and retrievals," *Atmos. Meas. Tech.*, vol. 6, pp. 2359–2372, 2013.

[24] J. Wang and L. Zhang, "Systematic errors in global radiosonde precipitable water data from comparisons with ground-based GPS measurements," *J. Clim.*, vol. 21, pp. 2218–2238, 2008.

[25] J. E. M. Goldsmith, F. H. Blair, S. E. Bisson, and D. D. Turner, "Turn-key Raman lidar for profiling atmospheric water vapor, clouds, and aerosols," *Appl. Opt.*, vol. 37, no. 21, pp. 4979–4990, Jul. 1998.

[26] S. G. Benjamin *et al.*, "2006 TAMDAR impact experiment results for RUC humidity, temperature, and wind forecasts," in *Proc. 11th Symp. Integr. Observ. Assimilation Syst. Atmos. Oceans Land Surf.*, San Antonio, TX, USA, 2007, pp. 1–9.

[27] U. Löhnert, S. Crewell, and C. Simmer, "An integrated approach toward retrieving physically consistent profiles of temperature, humidity, and cloud liquid water," *Amer. Meteorol. Soc.*, vol. 43, pp. 1295–1307, Sep. 2004.

[28] A. S. Milman, *Mathematical Principles of Remote Sensing: Making Inferences from Noisy Data*. Boca Raton, FL, USA: CRC Press, 2000.

[29] J. Randa *et al.*, "Recommended Terminology for Microwave Radiometry," Nat. Inst. Standards Technol., Gaithersburg, MD, USA, NIST Tech. Note TN1551, 2008.

[30] T. J. Hewison, *Profiling Temperature and Humidity by Ground-based Microwave Radiometers*. Reading, MA, USA: The Univ. Reading, 2006.

[31] J. J. Braun and C. Rocken, "Water vapor tomography within the planetary boundary layer using GPS," in *Proc. Int. Workshop GPS Meteorol.*, Tsukuba, Japan, 2003, pp. 3-09-1–3-09-4.

Swaroop Sahoo received the B.Tech. degree in electrical engineering from Biju Pattnaik University of Technology, Bhubaneswar, India, in 2005, and the M.S. degree in electrical engineering from Colorado State University, Fort Collins, CO, USA, in May 2011. Currently, he is working toward the Ph.D. degree in electrical engineering at Colorado State University.

Xavier Bosch-Lluis received the Master's degree in telecommunication engineering specialized in communications systems, in 2005, the Master of Science degree in research on information and communication technologies (MERIT) in 2007, the Master's degree in electronics engineering in 2010, and the Ph.D. degree in signal theory and communications from the Universitat Politècnica de Catalunya (UPC), Barcelona, Spain, in March 2011.

Since April 2011, he has been a Post-Doctoral Researcher with the Microwave Systems Laboratory, Electrical and Computer Engineering Department, Colorado State University, Fort Collins, CO, USA. His research interests include developing innovative radiometer systems and retrieval algorithms for passive microwave and millimeter-wave remote sensing.

Steven C. Reising (S'88–M'98–SM'04) received the B.S.E.E. (*magna cum laude*) and M.S.E.E. degrees in electrical engineering from Washington University in St. Louis, Saint Louis, MO, USA, in 1989 and 1991, respectively, and the Ph.D. degree in electrical engineering from Stanford University, Stanford, CA, USA, in 1998.

Currently, he is a Full Professor in Electrical and Computer Engineering with Colorado State University (CSU), Fort Collins, CO, USA, since July 2011, where he served as an Associate Professor from August 2004 to June 2011. Before joining the CSU faculty in 2004, he served as an Assistant Professor in Electrical and Computer Engineering with the University of Massachusetts Amherst, Amherst, MA, USA, where he received tenure. He served as a Summer Faculty Fellow for three summers in the Remote Sensing Division, Naval Research Laboratory, Washington, DC, USA. He has been the Principal Investigator of more than 12 grants from the National Science Foundation (NSF), NASA, Office of Naval Research (ONR), NPOESS Integrated Program Office, European Space Agency, and Ball Aerospace and Technologies Corporation. His research interests include broad range of remote sensing disciplines, including passive microwave and millimeter-wave remote sensing of the oceans, atmosphere, and land; microwave circuits and radiometer systems; lidar systems for sensing of temperature and winds in the middle and upper atmosphere; atmospheric electrodynamics; low-frequency remote sensing of lightning; and its energetic coupling to the ionosphere, which produces chemical changes and transient optical emissions.

Dr. Reising serves as the Vice President of Information Resources (2011–present) and formerly as the Vice President of Technical Activities (2008–2010) of the IEEE GEOSCIENCE AND REMOTE SENSING SOCIETY (GRSS). He has served as an elected member of the IEEE Microwave Theory and Techniques Society (MTT-S) Administrative Committee (AdCom) since January 2014, for which he is currently a Technical Coordinating Committee Vice-Chair and Outstanding Chapter Award Co-Chair. He has served as an elected member of the IEEE GRSS AdCom continuously since 2003, after 3-year term as an Editor of the GRSS Newsletter (2000–2002) and Associate Editor for University Profiles (1998–2000). He was an Associate Editor of the IEEE TRANSACTIONS ON GEOSCIENCE AND REMOTE SENSING LETTERS (GRSL) from its founding in 2004–2013. He has been a Guest Editor of IEEE TRANSACTIONS ON GEOSCIENCE AND REMOTE SENSING (TGRS) for the International Geoscience and Remote Sensing Symposium (IGARSS) 2012 Special Issue published in September 2013, the IGARSS 2008 Special Issue published in November 2009, and the Special Issue on Microwave Radiometry and Remote Sensing Applications published in July 2007. He has served as a Reviewer for TGRS, GRSL, the IEEE TRANSACTIONS ON MICROWAVE THEORY AND TECHNIQUES, *Remote Sensing of Environment, the Journal of Atmospheric and Oceanic Technology, the Journal of Geophysical Research—Oceans, Geophysical Research Letters, Marine Geodesy, Atmospheric Chemistry and Physics, the Journal of Oceanography, and Radio Science*. In organizing scientific meetings, he was one of two Technical Program Co-Chairs of the IEEE IGARSS 2008 in Boston, MA, USA, with over 1700 attendees. He served as the General Chair of MicroRad'06, the 9th Specialist Meeting on Microwave Radiometry, held in March 2006 in San Juan, Puerto Rico, with 126 attendees from 15 countries. He was the Local Arrangements Chair for IGARSS 2006 in Denver, with over 1250 attendees. He has been an active participant in each IGARSS Technical Program Committee from 2001 to the present. He serves the URSI as the Chair (2012–2014) and previously as Secretary and Chair-Elect (2009–2011) of its USNC, consisting of 10 scientific commissions focusing on the theory and applications of electromagnetics and radio waves from ultra-low frequencies to terahertz. He chaired the first three URSI International Student Paper Prize Competitions at the URSI General Assemblies and Scientific Symposia held in Chicago, Illinois in 2008; Istanbul, Turkey in 2011; and Beijing, China in 2014. Previously, he chaired the annual USNC-URSI Student Paper Prize Competition at the National Radio Science Meeting in Boulder each year from 2004 to 2008 and at the URSI North American Radio Science Meeting, Ottawa, ON, Canada, in 2007. In addition, he has served as Technical Program Co-Chair for the USNC-URSI National Radio Science Meetings held each January in Boulder, CO, USA, from 2010 to 2014. He served as the Secretary of USNC-URSI Commission F (2006–2008) and is a member of URSI Commissions F, G, and H, the American Meteorological Society, the American Geophysical Union, Tau Beta Pi, and Eta Kappa Nu. He was the recipient of the NSF CAREER Award (2003–2008) in the areas of physical and mesoscale dynamic meteorology and the ONR Young Investigator Program Award (2000–2003) for passive microwave remote sensing of the oceans. He was the recipient of the Barbara H. and Joseph I. Goldstein Outstanding Junior Faculty Award in 2004, the Lilly Teaching Fellowship for 2001–2002, and a Young Scientist Award at the URSI General Assembly, Toronto, Canada, in 1999. While at Stanford, he received first place in the United States National Committee (USNC) of URSI Student Paper Competition at the 1998 National Radio Science Meeting, Boulder, CO, USA.

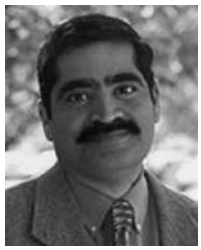

Jothiram Vivekanandan (M'05–SM'10) received the B.E. degree in electronics and communications engineering from Madurai Kamaraj University, Madurai, India, the M.Tech. degree in microwave and radar engineering from the Indian Institute of Technology, Kharagpur, India, and the Ph.D. degree in electrical engineering from Colorado State University, Fort Collins, CO, USA, in 1986.

He holds a Senior Scientist appointment in both the Earth Observing Laboratory and the Research Applications Laboratory, National Center for Atmospheric Research (NCAR), Boulder, CO, USA. He is an Associate Editor of Radio Science. His research interests include the interpretation of remote sensing instruments' responses to clouds and precipitation using mathematical models and actual field observations.